

Chung-Hao Chen (陳中皓)*, Ting-Heng Hsieh (謝廷珩), Hong-Yue Huang (黃宏岳),
 Yu-Chan Cheng (鄭又鈞), and Tzay-Ming Hong (洪在明)
 Department of Physics, National Tsing Hua University, Hsinchu 30043, Taiwan, Republic of China
 * zhonghaophys@gmail.com, cellphone: 0908911723

ABSTRACT

The unique ability of fire ants to form a raft to survive flooding rain has enchanted biologists as well as researchers in other disciplines[1-3]. In addition to clarifying that Cheerios effect [4] is neither sufficient nor essential for the ant raft, we perform the force-displacement and creep experiments on the ant raft and concentrate on unearthing properties that derive from the unique combination of self-healing and activeness of its constituent. Varying the pull speed results in distinct mechanical responses and fracture patterns, characteristic of ductile and brittle material. In addition, the raft can be tailored not to transversely deform in response to the axial strain. Without resorting to specific geometry structures, this property of zero Poisson's ratio is enabled by the active recruitment of ants from the top to bottom layer to keep the raft from disintegrating. Furthermore, effective Young's modulus can also be customized and is proportion to either the raft length or its inverse, depending on whether the raft is in the elastic or plastic region.

Experimental setup

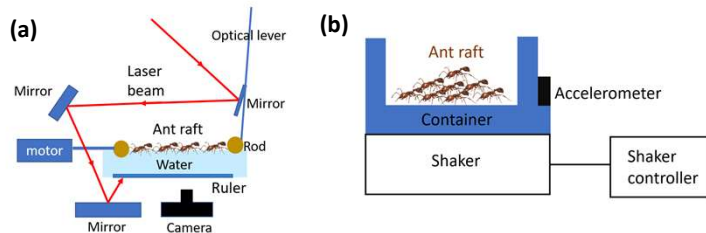


FIG. 1. (a) Schematic experimental setup for measuring the mechanical and creep properties of fire ant raft. (b) A shaker is employed to test whether flooding is the only means to induce the action of aggregation for fire ants. Note that ants never touch the wall when jiggled horizontally. The container is coated with teflon (Chemours DISP 30) to avoid fire ants from gripping and escaping. Side and top views of fire ants, local ants and dead fire ants under different environments to facilitate aggregation.

Ant rafts formed by different means

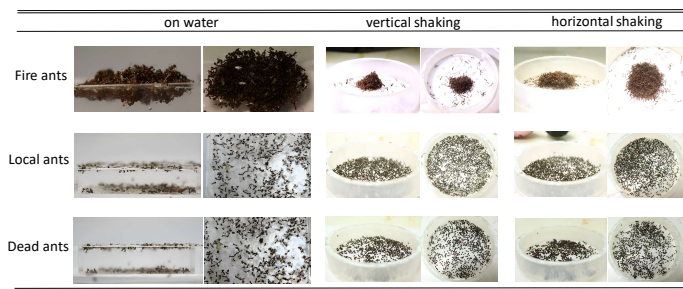


TABLE. 1. Side and top views of fire ants, local ants and dead fire ants under different environments to facilitate aggregation.

Force-displacement experiment

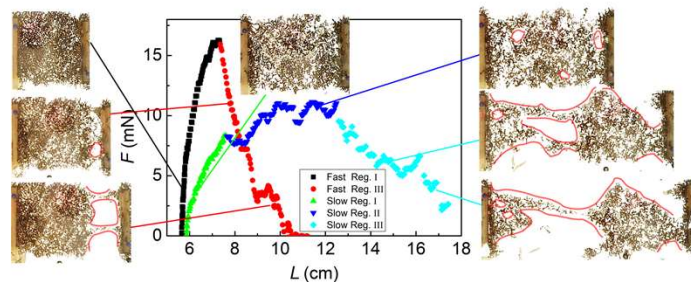


FIG. 2. The pull force versus length of ant raft under fast (1.7 mm/s) and slow (0.25 mm/s) pull speeds. Representative snapshots for each region are shown. Red curves are used to highlight the cracks developed in the interior and at the edge of the ant raft. In contrast to being stationary in region II, these cracks expand irreversibly upon entering region III. Note that region II is missing for high pull speed.

Conclusion

By showing that local ants and dead fire ants do not aggregate on water, we demonstrate that the ascription of fire ant raft to the Cheerios effect is not sufficient. Neither is it necessary because fire ant raft can also be formed by shaking vertically or horizontally. By doing the force-displacement experiment, we found that fire ant raft behaves like a brittle material when pulled fast, but becomes ductile if pulled slowly. By image processing, we were able to count the number of ants whose orientations are aligned with the pull force, which is strongly correlated with the magnitude of force when pulled slowly. In the creep experiment, zero Poisson's ratio is found in Slow and Fast Reg. I-II, and effective Young's modulus is proportional to the inverse power of length in Slow Reg. I-II and the power of length in Fast Reg. I-II.

Analogy to lamellae phase in liquid crystal

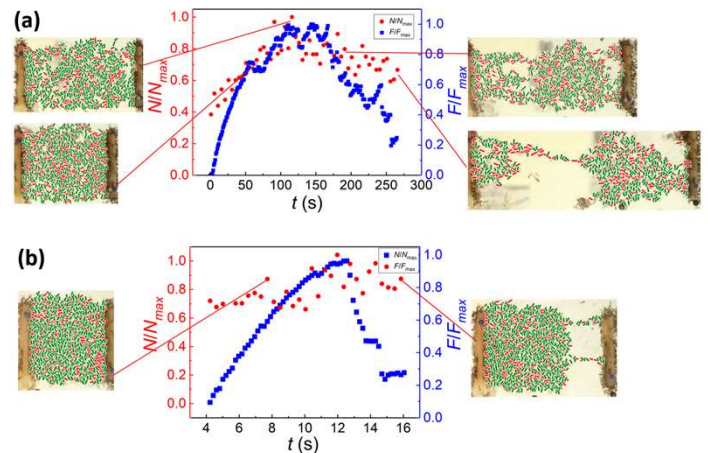


FIG. 3. In order to capture how the number of aligned ants N correlated with the pull force F , they are plotted in double Y-axis graphs as a function of time. Both quantities are rescaled by their maximum value to facilitate comparison. (a) and (b) are respectively for low and high pull speed. Alignment is defined by an deviation less than 20° between the ant orientation and the pull direction. These ants are marked by red lines in the photos, otherwise in green.

Creep experiment

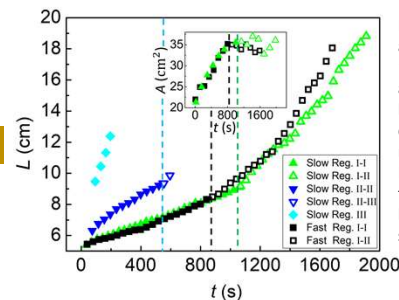


FIG. 4. The creep experiment 1: Length L of ant raft relaxes under a constant $F = 2.46, 13.43$ and 8.93 mN for Slow Reg. I, II and III, and 3.4 mN for Fast Reg. I. The blue dashed line denotes the transition for Slow Reg. II-III data, i.e., for a slow pull speed and from region II to III. Likewise, yellow is for Fast Reg. I-III, and red is for Slow Reg. I-II. Inset shows the change of morphology for yellow and red lines is accompanied by an approximate saturation of raft area, A

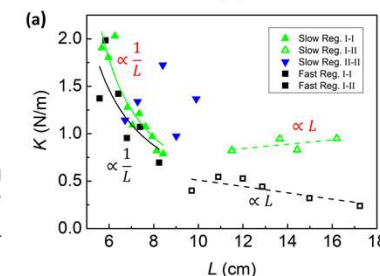


FIG. 5. The creep experiment 2: (a) Effective spring constant K is plotted against L in Fig. 3. Except for Slow Reg. II-II, the other four data are fitted respectively by solid ($1/L$) and dashed (L) green lines for slow speed, and the same in black for fast speed. Although roughly observing the increasing trend as Slow Reg. I-II, the data of Slow Reg. II-II fluctuate wildly due to the fact that we are forced to adopt a smaller ΔF to avoid hastening the raft into region III. This increases the uncertainty in ΔL . Snapshots of Slow and Fast Reg. I-II rafts are shown in (b) and (c). Note that the neck in (c) is not only narrower than that in (b), but its width also shrinks faster.

Reference

[1] D. J. Pearce *et al.*, Proc. Natl. Acad. Sci. U.S.A. **111**, 10422 (2014).
 [2] W. Bialek *et al.*, Proc. Natl. Acad. Sci. U.S.A. **109**, 4786 (2012).
 [3] H. H. Mattingly and T. Emonet, Proc. Natl. Acad. Sci. U.S.A. **119**, e2117377119 (2022).
 [4] H. Ko, M. Hadgu, K. Komilian, and D. L. Hu, Phys. Rev. Fluids **7**, 090501 (2022).